

Risk Assessment of Fatigue Cracks in Corroded Lap Joints

Alan P. Berens

University of Dayton Research Institute
Dayton, Ohio 45469-0120 USA

J. Doug West and Angela Trego

Boeing Defense & Space Group
P.O. Box 7730 MS K86-74
Wichita, Kansas 67277-7730 USA

1. SUMMARY

As part of a program to develop analytical tools for predicting and validating the effects of corrosion on fatigue life assessments, deterministic crack growth predictions were made for a test specimen that is representative of a transport fuselage lap joint. Fatigue tests had been performed using this specimen and the results were made available by the National Research Council of Canada. The test data provided the necessary information to define boundary conditions, cracking scenarios, and initiating crack size distributions as well as to validate predictions. In addition to corrosion severity, which was modeled by the metric of uniform material thinning, the crack growth predictions also had to account for multiple site damage.

This paper uses the lap joint specimen test data and the deterministic crack growth predictions to demonstrate a risk analysis approach for quantifying random effects of factors associated with corrosion damage. Stress intensity factors and crack growth are calculated for selected percentiles of assumed distributions of corrosive thinning. Output from these deterministic analyses are then used in the risk analysis program PRobability Of Fracture (PROF) to calculate conditional failure probability as a function of experienced cycles for the multiple sets of defined conditions. The results are interpreted by a comparison of risks for the various degrees of thinning and by an implied distribution of hours to reach a fixed failure probability for the assumed distributions of corrosive thinning.

2. INTRODUCTION

Fatigue crack growth predictions are at the core of damage tolerance analyses of metallic structures. To date, these predictions have been based on design geometries and material properties and do not account for the degradation associated with corrosion.

Modeling tools and data are now being developed that will permit deterministic predictions of fatigue crack initiation and crack growth life in corroded structure. However, the severity and extent of corrosion and the unknown state of fatigue damage in aging aircraft are stochastic effects that must somehow be accounted for in the planning of inspections, repairs, and replacements. The traditional approach to accounting for random variation in life influencing factors is to make conservative assumptions that cover the expected scatter. In recent years, risk analysis has seen increasing use as an additional fleet management tool that directly addresses the stochastic nature of structural integrity [1, 2, 3].

Structural risk analysis is based on the probability of failure in a defined population of structurally significant details. In a fatigue environment, this probabilistic evaluation of strength versus stress is dynamic since strength degrades as fatigue cracks initiate and grow. Fracture mechanics provides deterministic tools that predict the growth of cracks for fixed stress sequences from an initial size to critical size. By introducing probabilistic descriptions of the factors that produce different initiating conditions and crack growth in the population, the results from deterministic tools can be extended to quantify the degree of safety during an operating period by calculating the probability of failure of a structural element as a function of time.

The objective of this paper is to demonstrate that risk analyses can also include a probabilistic description of corrosion severity. Failure probabilities are calculated using the computer program PRobability Of Fracture (PROF) which is based on deterministic damage tolerance analysis data and an initiating distribution of crack sizes in the population of details. The demonstration uses crack growth predictions and

initiating data from a test program on a lap joint specimen that is representative of a cargo/transport airframe. A simple probabilistic description of multiple site damage (MSD) is also included in the example.

3. RISK METHODOLOGY

The risk analysis methodology of this paper uses a fracture mechanics based program, PROF, that was formulated for United States Air Force applications. The program uses the stress and crack growth data that are known to be available for all critical locations of structurally significant details because of the USAF Aircraft Structural Integrity Program. In PROF, the distribution of crack sizes at a critical location is grown by projecting the percentiles of the distribution in accordance with the calculated crack size versus flight time history for the anticipated stresses. Provision is made for updating the crack size distribution at inspection and repair intervals. A single run of PROF calculates the probability of failure as a function of flight hours from the joint distribution of crack sizes, maximum stress per flight, and fracture toughness. PROF input and output is presented in schematic form in Figure 1. See [4] for a complete description of the program and [3, 5, 6] for example applications.

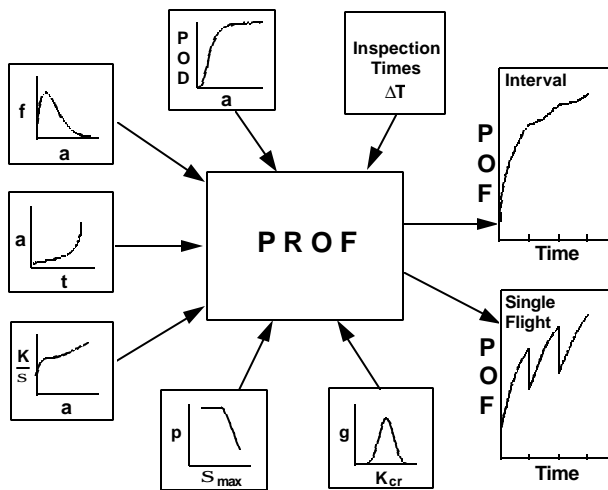


Figure 1. Schematic of PROF Calculation of Failure Probability

A single run of PROF produces failure probabilities for the specific population of details being modeled by the geometry and anticipated stresses of the deterministic crack growth model. For example, regions of equivalent stress and geometries are often

identified for stress raisers in a fleet of aircraft. When the initiating crack size distribution is representative of all cracks that are present in the stress raisers in the fleet, the failure probabilities would be applicable to a randomly selected airframe from the fleet. There are many structural details for which this calculation is directly relevant and, in fact, decisions to change inspection schedules have been influenced by such risk calculations. However, there are also many structural details for which the conditions are not constant across an entire fleet and the effect of these conditions can be modeled through multiple runs of PROF.

The total population of details is divided into sub-populations of equivalent stresses and geometries. Conditional failure probabilities are calculated for each sub-population. The conditional probabilities can be directly interpreted in terms of the sub-population represented by the conditions. When the relative frequencies (probabilities) of the conditions are also known, the conditional fracture probabilities can be combined to provide an overall fracture probability as a function of time. This calculation is given by

$$POF(T) = \sum POF(T/C_i) \cdot P(C_i) \quad (1)$$

where $POF(T/C_i)$ is the probability of failure at T given that condition C_i was used to determine the crack life of the structure and $P(C_i)$ is the probability that condition C_i applies and $\sum P(C_i) = 1$.

To illustrate this concept, consider the lap joint risk analysis that will be demonstrated in this paper. The population of lap joint specimens to be analyzed will be divided into sub-populations based on combinations of MSD scenarios and corrosion severity levels. Cracking occurred in dominant MSD scenarios whose influence on crack growth was exhibited through the stress intensity factor. Corrosion severity was characterized by the metric of uniform thickness loss whose influence on crack growth is exhibited through the experienced stress levels. Each combination of MSD scenario and thickness loss produces a different crack growth analysis so that each combination must be individually analyzed in the risk analysis. In this paper, two dominant MSD scenarios were judged sufficient to model the life determining lead cracks in the lapjoint. Five degrees of uniform thickness loss were assumed to represent degrees of corrosion severity.

		Dominant MSD		
Corrosion Severity	Proportion of Joints	Scenario 1 p_1	Scenario 2 p_2	Composite over MSD
Thickness Loss 1	q_1	$POF_{11}(T)$	$POF_{21}(T)$	$p_1POF_{11}(T)+p_2POF_{21}(T)$
Thickness Loss 2	q_2	$POF_{12}(T)$	$POF_{22}(T)$	$p_1POF_{12}(T)+p_2POF_{22}(T)$
Thickness Loss 3	q_3	$POF_{13}(T)$	$POF_{23}(T)$	$p_1POF_{13}(T)+p_2POF_{23}(T)$
Thickness Loss 4	q_4	$POF_{14}(T)$	$POF_{24}(T)$	$p_1POF_{14}(T)+p_2POF_{24}(T)$
Thickness Loss 5	q_5	$POF_{15}(T)$	$POF_{25}(T)$	$p_1POF_{15}(T)+p_2POF_{25}(T)$

$POF_{ij}(T) = POF(T/S_i, L_j)$ = Probability of failure for Scenario i, Thickness Loss j

p_i = Proportion of lap joints with crack initiating under Scenario i

q_j = Proportion of lap joints with uniform thickness loss at level j

Figure 2. Conditional Failure Probabilities for 2 MSD Scenarios and 5 Levels of Uniform Thickness Loss

Figure 2 illustrates the partitioning of the total population of the lap joints into the ten sub populations. Every lap joint must fit into one of the sets of conditions defined by MSD scenario and thickness loss. The probability that cracks will initiate under Scenarios 1 and 2 are p_1 and p_2 , respectively. The probability that a randomly selected lap joint will have uniform thickness loss level j is q_j . $POF(T/S_i, L_j) = POF_{ij}(T)$ is the probability of fracture as a function of time for the combination of MSD Scenario i and Thickness Loss j. The calculation of the unconditional probability of failure for a random lap joint in the fleet for each corrosion severity level is shown in the last column. An analogous calculation could be performed across severity levels to obtain composite failure probabilities for each MSD scenario.

An interpretation of the corrosion effects can be made directly from the PROF output. If an estimate of the distribution of thickness loss in the fleet is also available, the results of the individual runs of PROF can be combined using Equation (1) to provide an overall fracture probability for a randomly selected detail. Further, the distribution of time to reach a fixed fracture probability can be inferred from the percentiles associated with the corrosion severity levels. These analyses will be demonstrated for corrosion in a representative lap joint.

It is realized that the risk analysis reported herein does not account for the stress levels increasing as a result of increasing corrosion over the analysis period. At present, there are no accepted models for the

corrosion damage growth (thickness loss) as a function of time so that the crack growth calculations are based on the state of corrosion at the beginning of the analysis interval. In reality, the stresses in the spectrum should be slowly increasing. If this effect could be accounted for in the deterministic analysis, the crack growth data input to PROF would reflect the change. However, the peak stress distribution would need to be made more severe at discrete increments. This added complexity could be performed by performing multiple PROF runs. It might be noted that in the lap joint example of this paper, the peak stress distribution had no effect on the failure probability. The failure of the joint specimen was determined by reaching an unstable crack growth state when the lead crack reached a fixed size that was far below the critical crack size for the applied far field stress.

4. LAP JOINT CORROSION EXAMPLE

As part of a program to develop an analytical corrosion damage assessment framework [7], crack life predictions were made for a lap joint specimen to verify the prediction methodology. The lap joint specimens had been used in a fatigue test program by Carleton University and the National Research Council (NRC) of Canada [8,9]. The specimen, Figure 3, is constructed of two 1mm sheets of 2024-T3 clad aluminum with three rows of 4mm 2117-T4 rivets (MS20426AD5-5). The rivet pattern has 25.4mm pitch and row spacing with an edge margin of 9.1mm. The test specimens were 25.4cm wide with 8 fasteners in each row across the width.

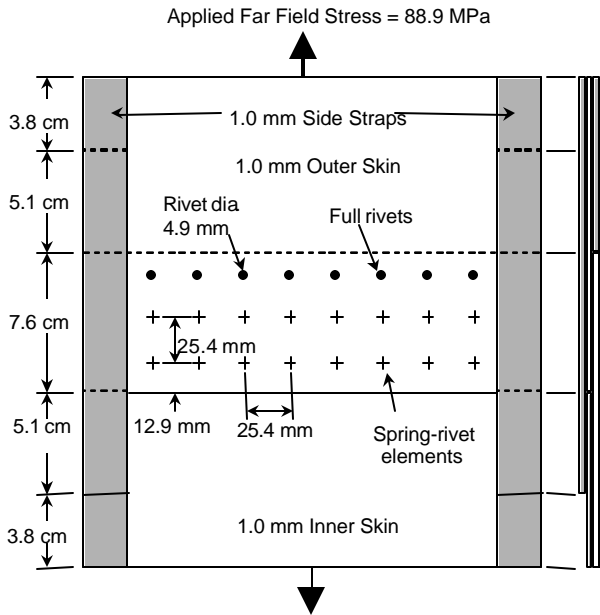


Figure 3. Schematic of Lap Joint Specimen

Constant amplitude fatigue tests had been conducted at Carleton University on the lap joint specimens in non-corroded and corroded conditions with a constant amplitude far field stress of 88.9 MPa with $R = 0.2$. Details of the test procedure and resulting fatigue crack growth data are presented in [8]. Nine non-corroded specimens were tested to failure to provide baseline data for comparison with corrosion specimens. Only data from these non-corroded baseline specimen tests are used in this paper. Histories of crack size versus cycles for all cracks that initiated in the top row of rivet holes were available for analysis. Examination of the histories showed that 95 percent or more of the joint life was expended when the lead crack reached about 9mm and crack growth became unstable. Further, lead cracks initiated in accordance with two dominant scenarios. In Scenario 1, a single crack originated from one side of a central hole. In Scenario 2, approximately simultaneous, diametric cracks originated from both sides of a central hole. Subsequent analysis showed significantly shorter lives for the double initial cracks. Analysis also showed that assuming both cracks were of equal size produced only 5 percent shorter lives than assuming one crack was twice the size of the second. Consequently, the assumptions were made that: a) joint life is determined by the initiation and growth of lead cracks that originate by one of two scenarios; b) the cracks are of equal size in the double crack scenario, and, c) the panel is essentially failed when the lead crack reaches 9mm.

Because first cracks were simultaneously discovered in different holes in four of the nine data sets, there were a total of 13 lead cracks. Eight were from Scenario 1 and five were from Scenario 2. For this population of structural elements, it was assumed that probability of a randomly selected lap joint having a Scenario 1 lead crack was $8/13$ and the probability of a randomly selected lap joint having a Scenario 2 lead crack was $5/13$.

Crack growth analyses were performed for both scenarios [10]. Stress analysis was performed using FRANC2D/L, a finite element, fracture mechanics analysis code with crack propagation capability [11, 12]. The resulting crack tip stress intensity factor values as a function of crack size were then input to the crack growth code AFGROW [13] for selected degrees of corrosion severity. The no corrosion, constant amplitude peak stress of the baseline fatigue tests and crack growth analyses was 88.9 MPa with an R ratio of 0.2. Predicted cyclic life from 0.25mm to 9mm averaged about 30 percent more than the test data.

Corrosion severity was modeled in terms of percent of thinning with the attendant increase in stress. To reflect corrosion severity, crack growth predictions were made for the somewhat arbitrarily selected levels of 2, 5, 8, and 10 percent corrosive thinning by proportionate adjustments of the stress levels.

5. RISK ANALYSIS (PROF) INPUT

The risk analysis for the lap joint corrosion example requires ten individual runs of PROF – two MSD scenarios and five stress levels for each of the MSD scenarios. The most significant inputs for the runs of this lap joint example are the crack growth projections and the initial crack size distribution. The other PROF inputs that reflect the changes between runs are the table of stress intensity factor divided by stress (K/σ) as a function of crack size and the distribution of peak stresses. These were changed between runs even though they had no affect on the results. K/σ came from the FRANC2D/L analysis. The peak stress distribution was estimated by a Gumbel extreme value distribution that had a mean at the appropriate constant amplitude level and a very small standard deviation to reflect the constant amplitude nature of the tests. Fracture toughness for the specimen was assumed to be normally distributed with a mean and standard deviation of 152 and 11.4 $\text{Mpa}\sqrt{\text{m}}$, respectively. Because the example being modeled does not include inspection and repair

cycles, reasonable, but arbitrary, data were used to define the inspection capability and the equivalent repair flaw size distributions.

The AFGROW crack growth curves for Scenarios 1 and 2 are presented in Figures 4 and 5, respectively. Each figure contains five crack growth curves reflecting the five levels of corrosion severity. The shorter crack growth lives from Scenario 2 are apparent from a comparison of these figures.

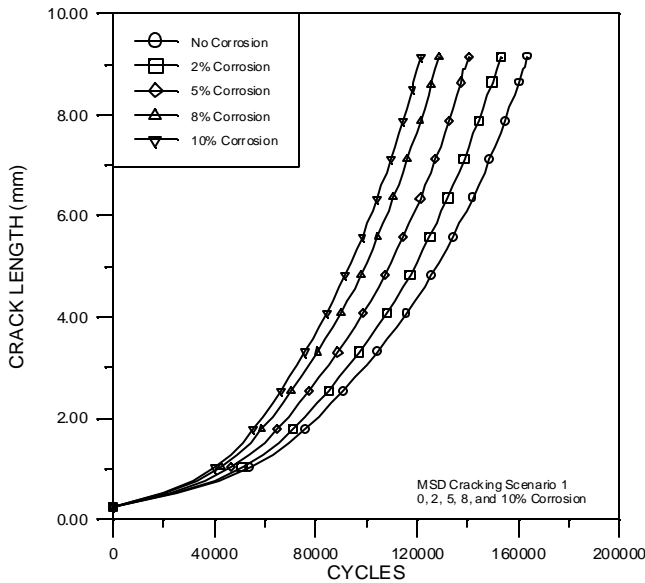


Figure 4. Crack Size versus Cycles for Scenario 1

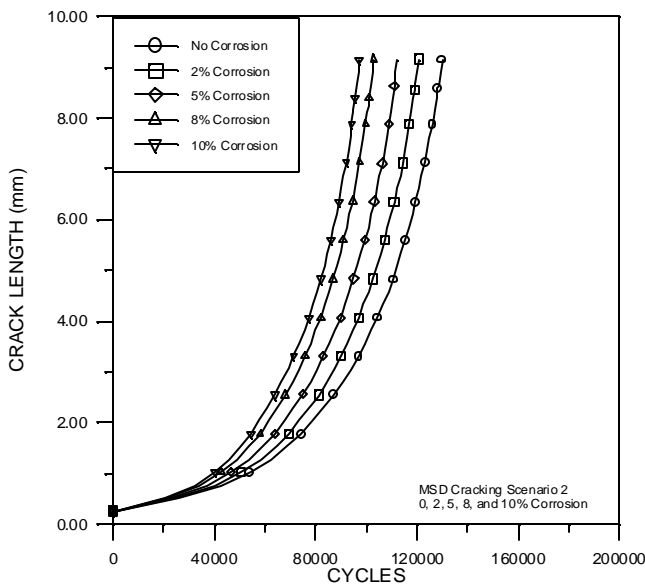


Figure 5. Crack Size versus Cycles for Scenario 2

The initiating flaw size distribution was generated by back calculating from the sizes of the first observed lead cracks and their corresponding ages in the specimen test data. The back calculation was performed in two steps. First the no corrosion crack size versus cycles data of Figures 4 and 5 were used to determine the time at which each lead crack would have reached 0.25mm. An exponential growth model was then fit to each lead crack to estimate an equivalent crack size at 50,000 cycles. The extrapolation process for the lead crack sizes is shown in Table 1. Note that the inverse of this process returns each of the observed lead cracks to its original size and cycles.

Table 1. Extrapolation for Initiating Flaw Size Distribution

Scenario 1 - Single Crack on Side of Rivet Hole					
ID	Size at 1 st	Cycles 1 st Obs.	Cycles at c=0.25m	B=2.76e-A**	Size at 50000**
F1-4R	2.49	291955	202297	9.60E-04	3.81E-
F1-3R	0.74	291955	251938	2.45E-04	9.70E-
F3-5L	1.45	175000	107493	1.31E-02	5.20E-
F4-4L	2.74	195000	100638	1.58E-02	6.29E-
F6-4L	0.46	385000	364914	1.08E-05	4.31E-
F7-4R	0.89	208006	160214	3.07E-03	1.22E-
F9-5R	1.09	130103	73559	3.35E-02	1.33E-
F9-4L	1.80	135000	58939	5.00E-02	1.99E-
Scenario 2 - Double Cracks of Equal Lengths at Rivet					
ID	Size at 1 st	Cycles 1 st Obs.	Cycles at c=0.25m	B=2.70e-A**	Size at 50000**
F6-	1.40	385000	319467	4.60E-05	1.77E-
F0-	1.98	336563	258737	2.37E-04	9.12E-
F5-	2.41	133000	48075	6.93E-02	2.67E-
F7-	2.06	201003	121787	9.53E-03	3.67E-
F8-	2.31	225000	141641	5.56E-03	2.15E-

* Translation from calculated c versus Cycles

** A = 0.25/exp(Cycles at 0.25 * B), B from 1st two points of

calculated c versus Cycles

*** c = A exp(B*Cycles)

The times to reach 0.25mm for the cracks from the two MSD scenarios were statistically indistinguishable. Similarly, there was no statistical difference between the equivalent lead crack sizes from the two MSD scenarios at 50,000 cycles. The two sets of data were pooled to obtain the initiating flaw size distribution. The equivalent crack sizes at 50,000 cycles were fit with a mixture of two Weibulls as shown in Figure 6.

Also indicated in Figure 6 are the MSD scenarios of origin of the lead cracks.

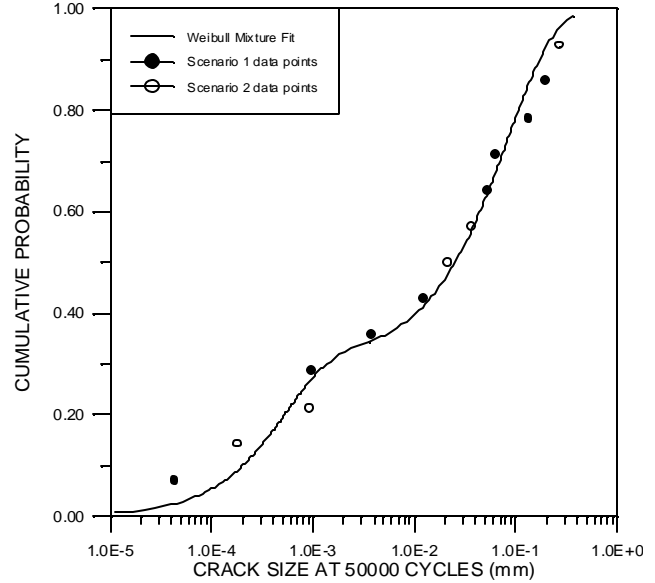


Figure 6. Weibull Mixture of Initial Crack Sizes

6. RISK ANALYSIS RESULTS

Probability of failure as a function of cycles was calculated for each of the ten combinations of cracking scenario and corrosion severity. Failure of the lap joint specimens was defined as the lead crack exceeding 9mm, as previously discussed. Figures 7 and 8 present the failure probabilities as a function of experienced cycles for Scenarios 1 and 2, respectively. The failure probabilities behave as expected with increased risk of failure at a fixed age for Scenario 2 as compared to Scenario 1 and increasing risk of failure as the stress level increases due to corrosion material loss. These calculations do not account for any additional corrosive thinning after the start of the analysis.

As a gross check on the capability of the risk analysis methodology, Figure 9 compares the calculated probability of failure as a function of cycles for 0% corrosion for Scenarios 1 and 2 to the observed distributions of failure times. Superimposed on the predicted failure probabilities are the observed cumulative distributions of the cycles to failure from the lap joints that were the basis of the analysis. The observed cumulative distribution function was obtained by ordering the cycles to failure and dividing the ranks of the ordered times by the sample size plus one. That is,

$$F(T_i) = i/(n+1) \quad (2)$$

where i is the rank for T_i , the time at which the i^{th} crack exceeded 9mm and n is the number of observed cracks that met the definition for the scenario. Sample sizes for Scenarios 1 and 2 were eight and five, as noted earlier. The differences between the observed and predicted probabilities of failure are most likely due to the conservative deterministic life predictions or the extrapolation of the crack size versus cycles relation that was required to obtain the initiating distribution of crack sizes.

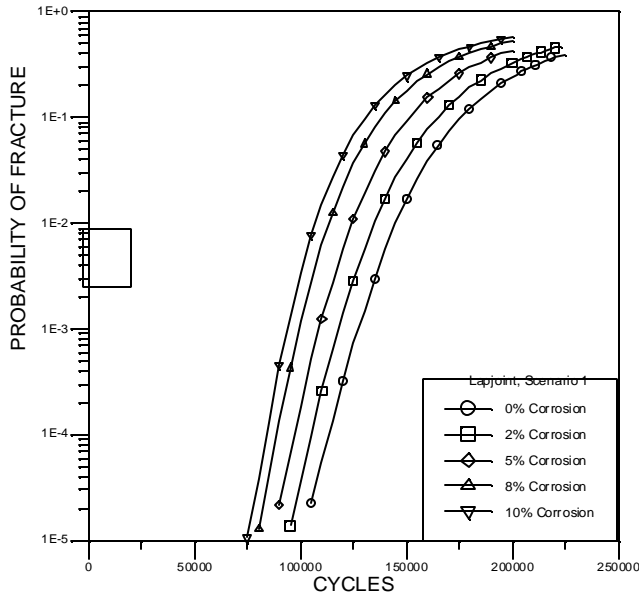


Figure 7. POF versus Cycles for Scenario 1

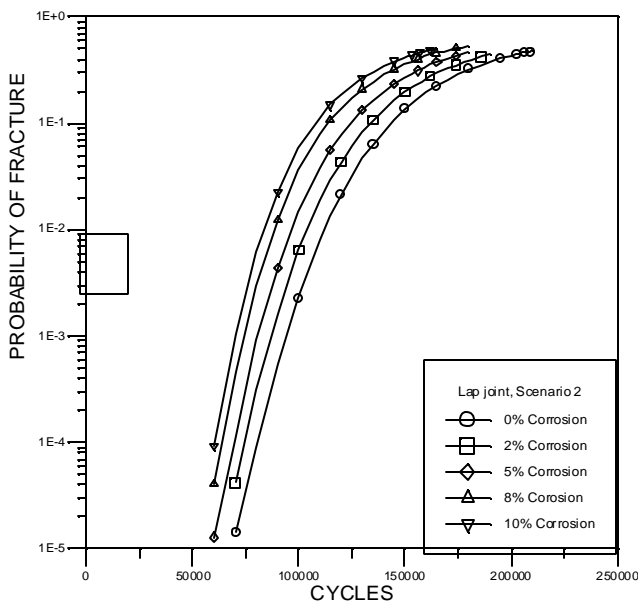


Figure 8. POF versus Cycles for Scenario 2

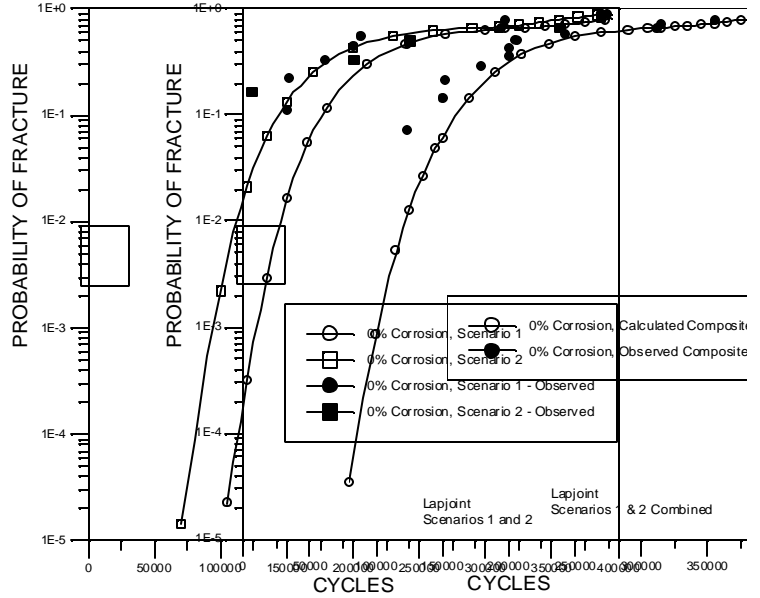
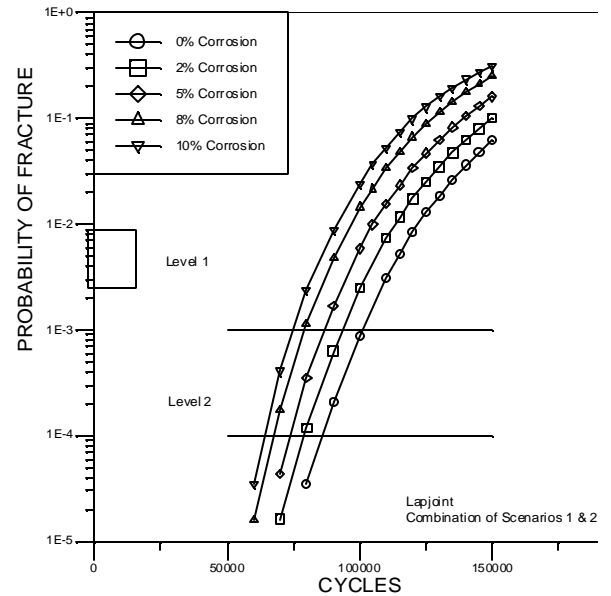


Figure 9. POF versus Cycles for Scenarios 1 and 2 Showing Comparison with Observed Data



Figures 7 and 8 present the conditional failure probabilities given the respective cracking scenario. The unconditional failure probability for a lap joint chosen at random from the population being analyzed is calculated as a weighted average of the conditional probabilities where the weighting factors are the proportion of specimens which will initiate cracks in the two scenarios. See Equation (1) and Figure 2. The weighting factors were estimated from the lap joint data in which 8 of the 13 lead cracks were from Scenario 1 (initial lead crack from one side of the

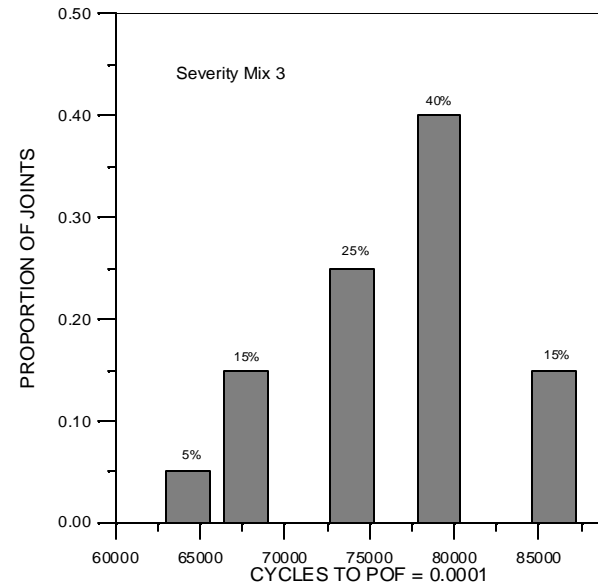
hole) and 5 of the 13 were from Scenario 2 (initial lead crack from diametrically opposite sides of the hole). Using these factors, a comparison of the observed and predicted cycles to failure for the composite of the two scenarios without corrosion is shown in Figure 10. Again the difference between the predicted and observed distributions of cycles to failure displays the somewhat non-conservative risks of the predicted failure probabilities.

Figure 11 summarizes the probabilities of failure for a randomly selected lap joint that can have either MSD scenario and is subject to the expected stress history for five levels of corrosion severity. These results will be interpreted both in terms of the times to reach a defined probability of fracture (POF) and in terms of the relative differences in POF at a fixed number of cycles.

Figure 10. POF versus Cycles for Composite of Scenarios 1 and 2 Showing Comparison with Observed Data

Figure 11. POF versus Cycles for Scenario Composites

The cycles to reach a fixed POF for the different degrees of corrosion severity can be read from Figure 11 as indicated, for example, at POF equal to 0.001 and 0.0001. Assume that the proportion of lap joints in the population that contain each of the five degrees of corrosion is known. Then the distribution of the



time to reach the POF levels can also be inferred. To illustrate, three representative distributions of corrosion damage were assumed, as given in Table 2. Mix 1 is symmetric about a five percent material loss. Mix 2 is representative of a more severely corroded population. Mix 3 is representative of a less severely corroded population and is considered to be more representative of the corrosion that would be expected in aircraft. Figure 12 presents a histogram of Mix 3. The corresponding percentage of lap joints would be expected to reach the selected POF level in the indicated number of cycles. The histogram for cycles to reach POF = 0.0001 for severity Mix 3 is shown in Figure 13. The cumulative distribution of time to reach the two POF levels for the three distributions of corrosion severity are shown in Figure 14.

Table 2. Representative Corrosion Level Damage Distributions

% Joints with Corrosion Severity			
Severity	Mix 1	Mix 2	Mix 3
0%	5	5	15
2%	20	15	40
5%	40	35	25
8%	25	35	15
10%	5	10	5

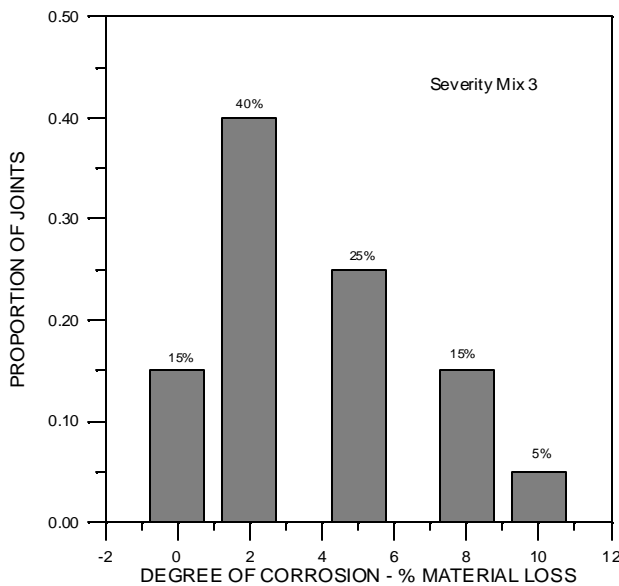


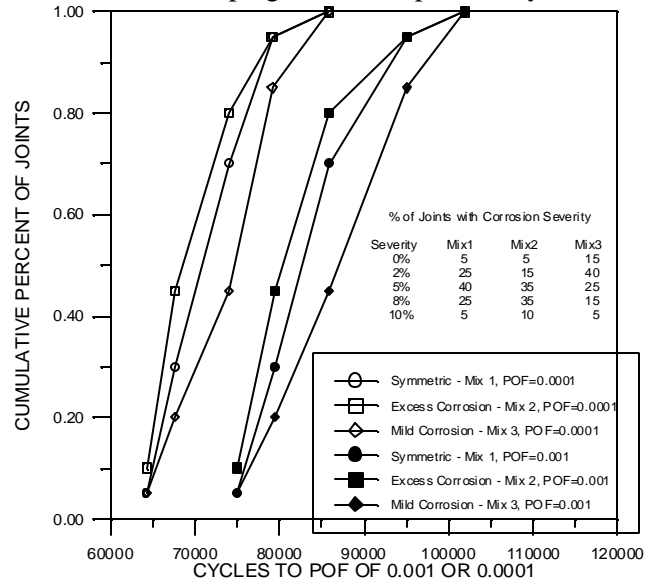
Figure 12. Example Histogram of Levels of Corrosion Damage – Severity Mix 3

Figure 13. Example Histogram of Cycles to POF = 0.0001 – Severity Mix 3

Figure 14. Cumulative Distributions of Cycles to Selected POF – 3 Corrosion Severities

At a fixed number of cycles, the failure risk of a corroded lap joint can significantly exceed that of a non-corroded lap joint. To illustrate this difference, Figure 15 presents the ratio of failure probabilities for each of the four degrees of corrosion severity to that of the non corroded lap joints. The ratios are presented as a function of the failure probability of the non corroded lap joint. The lap joint failure probability for the severity characterized by ten

percent thinning can be 70 times greater than that of a non corroded lap joint. If maintenance scheduling were based on keeping the failure probability below



about 0.0001 to 0.001, a lap joint with ten percent corrosion thinning would have a 25 to 50 times greater chance of resulting in fracture.

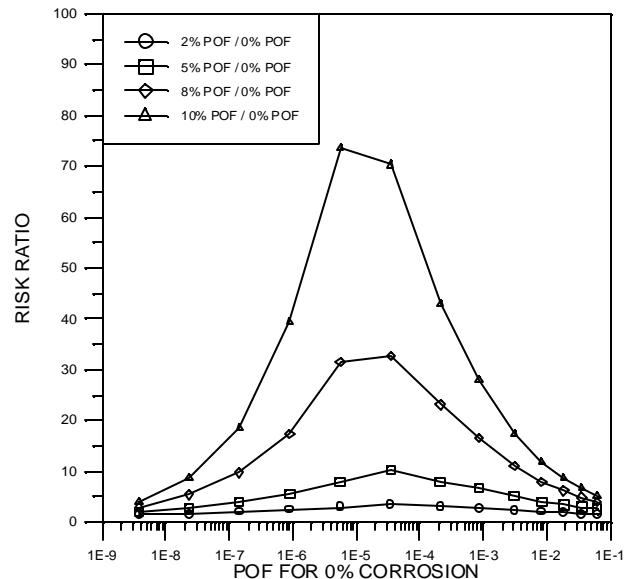


Figure 15. Risk Ratios Normalized to No Corrosion Condition

7. CONCLUSIONS

The use of risk analysis in structural maintenance planning recognizes that many life influencing factors may be unknown, and possibly unknowable,

for all equivalent details in an entire fleet. When acceptable conservative bounds cannot be determined for the condition of the higher order of importance factors, uncertainty in the characterization of the factors can be introduced in the form of distributions of severity. The risk analysis approach quantifies the degree of safety in terms of the likelihood of failure of the detail. The timing of maintenance actions can then be planned on the basis of keeping the probability of failure acceptably low or on the basis of minimizing ownership costs that also include the costs that are the result of unlikely, but possible, failures.

This paper demonstrates that it is possible to extend deterministic fracture mechanics crack growth results to include probabilistic descriptions of the factors which influence fatigue life. In particular, a risk analysis was performed for fatigue failures in a representative lap joint in which the crack growth calculation was influenced by corrosion thickness loss and two scenarios of MSD. The basic approach to the analysis is to use deterministic crack growth calculations for different percentiles of the influencing factors in the probability of failure calculations, yielding conditional probabilities of failure. The full use of the analysis assumes that estimates of the distribution of the influencing factors are available so that the conditional failure probabilities can be combined or otherwise interpreted.

In the lap joint example of this paper, the relative frequency of the two dominant MSD scenarios was estimated from data from a test program of the modeled specimen. Example distributions of thickness loss were assumed to demonstrate the calculations and interpretation. For this example, a ten percent thickness loss increased the failure probability by a factor of as much as 70 over the no corrosion condition. Depending on the consequences of failure, inspection intervals based on the no corrosion stress levels could pose a safety issue to corroded joints. The results were also used to demonstrate the generation of the distribution of time to a fixed risk.

The risk analysis calculations of this study are dependent on the quality of the deterministic crack growth analysis and the quality of the crack size data that characterize the damage state of the structural element. At present, crack growth modeling techniques which account for all of the complexities of corrosion damage are under development.

Further, data for characterizing the crack size distribution in a population is generally sparse.

8. REFERENCES

1. Lincoln, J.W., "Risk Assessments – USAF Experience," Proceedings of the International Workshop on Structural Integrity of Aging Airplanes, Atlanta, GA, 31 March – 2 April 1992.
2. Manning, S.D., Yang, J.N., and Welch, K.M., "Aircraft Structural Maintenance Scheduling Based on risk and Individual Aircraft Tracking," Theoretical Concepts and Numerical Analysis of Fatigue, A.F. Blom and C.J. Beevers, Eds., Engineering Materials Advisory Services, LTD, London, 1992, pp. 401-420.
3. Berens, A.P., "Applications of Risk Analysis to Aging Military Aircraft," SAMPE Journal, Vol. 32, No. 5, September/October 1996, pp. 40-45.
4. Berens, A.P., Hovey, P.W., and Skinn, D.A., "Risk Analysis for Aging Aircraft, Volume 1 – Analysis," WL-TR-91-3066, Air Force Research Laboratory, Wright-Patterson Air Force Base, Ohio, October, 1991.
5. Berens, A.P., "Risk Analysis Input for Fleet Maintenance Planning," Structural Safety and Reliability, Schueller, Shinozuka, and Yao (eds.), Balkema, Rotterdam, 1994.
6. Berens, A.P. and Burns, J.G., "Risk Analysis in the Presence of Corrosion Damage," AGARD - CP- 568, Widespread Fatigue Damage in Military Aircraft, NATO, Advisory Group for Aeronautical Research and Development (AGARD), Neuilly-Sur-Seine, France, December, 1995.
7. D500-13008-1 (1998). "Corrosion Damage Assessment Framework". The Boeing Company, Seattle, WA. Release date August 5, 1998.
8. Scott, J.P., "Corrosion and Multiple Site Damage in Riveted Fuselage Lap Joints," Master's Thesis, Carleton University, March 1997.

9. Eastaugh, G.F., Simpson, D.L., Straznicky, P.V., and Wakeman, R.B., "A Special Uniaxial Coupon Test Specimen for the Simulation of Multiple Site Fatigue Crack Growth and Link-Up in Fuselage Skin Splices," National Research Council of Canada and Carleton University, AGARD-CP-568, December 1995.
10. Trego, A., Cope, D., Johnson, P., and West, D., "Analytical Methodology for Assessing Corrosion and Fatigue in Fuselage Lap Joints," 1998 Air Force Corrosion Program Conference Proceedings, April 1998, Macon, Georgia.
11. Wawrzynek, P.A., and Ingraffea, A.R., "FRANC2D: A Two-Dimensional Crack Propagation Simulator, Version 2.7, User's Guide," NASA CR-4572, March 1994.
12. Swenson, D. and James, M., "FRANC2D/L: A Crack Propagation Simulator for Plane Layered Structures", Version 1.4 User's Guide, Kansas State University, December 1997.
13. Boyd, K., Harter, J.A., and Krishnan "AFGROW User's Manual Version 3.1.1," WL-TR-97-3053, Air Force Research Laboratory, Wright-Patterson Air Force Base, Ohio, February, 1998.